Use of aerofoil section dynamic stall synthesis methods in rotor design

W. Chan
wayland.chan@yahoo.co.uk
Aeroelastic Consultant
Yeovil, UK

J. Perry
Rotorcraft Consultant
Yeovil, UK

ABSTRACT

The introduction of the original time delay method of Beddoes, an engineering model for the unsteady response of an aerofoil section including dynamic stall, had a profound effect on the design and development of rotor systems in the UK. Over the years, the model expanded to include more and more features of the unsteady flow, with many contributors. It is now in use throughout the world as part of rotor analysis packages. Nevertheless, it retains its essential simplicity. Work to confirm the ability of the most recent version of the dynamic stall model from the University of Glasgow to replicate the complicated behaviour of an advanced rotor aerofoil section at full scale Reynolds and Mach numbers provides an opportunity to review the use of this new engineering model in the helicopter rotor design environment.

This note discusses the application of dynamic stall synthesis methods to the problem of classifying and comparing aerofoil sections when designing rotors for the retreating blade stall condition that determines the rotor blade area requirement of the helicopter. The development of the dynamic stall models employed in UK rotor designs is reviewed in this paper and their use in the design process explained, with emphasis on the assumptions that overcome the limitations of the models and exploit their simplicity, enabling accurate and conservative rotor designs. The paper shows how the model may be used to structure the analysis of complex sets

Paper No. 3707. Manuscript received 15 March 2011, revised version received 27 July 2011, second revised version received 28 November 2011, accepted 15 December 2011.
Paper originally presented at the HeliJapan 2010, Tokyo, Japan, 1-3 November 2010

https://doi.org/10.1017/S0001924000007004 Published online by Cambridge University Press

of dynamic aerofoil data. It illustrates how structured comparison between the model and the data yields a concise appreciation of the behaviour of the aerofoil and an understanding of the physical processes involved. Some previously unappreciated effects are identified and the model is used to transfer experience of the aerofoil section behaviour from the non-rotating wind-tunnel environment to that of the rotor. Finally, the application of the new engineering model developed at Glasgow University in the rotor design process is outlined. Some remarks on the use of engineering models in comparison with CFD models in the design context are included.

NOMENCLATURE

A_n, b_n	coefficients in aerofoil section indicial response relationship
c	aerofoil section chord
$C_{L\,MAX}$	aerofoil section maximum lift coefficient in static conditions
$C_{L\,1}$	aerofoil section equivalent maximum lift coefficient in dynamic conditions: $C_{L\,1} = C_{L\,\alpha}\,(\alpha_1 - \alpha_0)$
$C_{L\alpha}$	aerofoil section lift slope
C_N	aerofoil section normal force coefficient
K_θ	aerofoil pitch angular velocity
K_a	aerofoil rate of change of incidence
M	free stream Mach number
Re	Reynolds number
Δs_l	distance parameter used in the leading edge parameter stall calculation
t	time variable
T_n	time constants in aerofoil section indicial response relationship
U_p	peak leading edge velocity used in leading-edge parameter stall calculation
V	free stream velocity
α	aerofoil section incidence angle
α_0	zero lift incidence angle of aerofoil section
α_1	critical angle of incidence for initiation of stalling process, associated with aerofoil section pitching-moment break
$\Delta\alpha_E(t)$	change in effective aerofoil incidence (α) due to shed vorticity in wake
α_{LR}	angle for beginning of roll-off of lift – indicating the start of trailing-edge separation
α_{MB}	moment break angle derived from test
α'_{MB}	moment break angle corrected for trailing-edge separation
Δ	step change in incidence or time
θ	aerofoil section pitch angle
$\dot{\theta}$	aerofoil section rate of change of pitch angle

1·0 INTRODUCTION

When considering models for use in the engineering design and development process, requirements are considerably broader than the simple need for accuracy. Accuracy is important but so is cycle time for calculations. Calculations must keep pace with the design iteration process if they are to have any influence. Models used for design calculations should be simple in concept and based on the fundamental physics of the flow, so that they are quick and so that the trends they produce are readily understood.

https://doi.org/10.1017/S0001924000007004 Published online by Cambridge University Press

Traditional engineering models used to generalise or summarise experimental data or the results of more complex numerical calculations can fulfil these requirements. Since the best of these models amount to running summaries of the current understanding of the physical problems they describe, they may be used to guide the logic of design and development programs directly.

Good engineering models can be made to keep pace with developments in understanding as new data or calculations become available. Indeed, the intellectual activity required to keep the engineering model up to date provides the physical understanding required for design.

The treatment of aerofoil stalling under dynamic conditions by Beddoes[1] is an excellent example of an engineering model that can have a profound impact on the design and development process. The model itself has been steadily developed and reported over the years by various authors in various countries. This paper will concentrate on its impact on the design and development of helicopter rotors in the UK and, in particular, its use in structuring the logic of the design.

2.0 DISCUSSION

2.1 Dynamic stall on the retreating blade

The blade stalling process on the retreating side of a conventional helicopter rotor in high speed forward flight is central to the choice of rotor blade area and has a profound influence on the performance of the rotor and its weight. Blade stall is controlled by the stalling characteristics of the rotor blade aerofoil sections. When the rotor blade stalls, the resulting dynamic twisting or stall-flutter of the blades sets the aircraft flight envelope.

The introduction of the Beddoes' dynamic stall model and its incorporation into a rotor blade stall-flutter analysis e.g. Refs (1 and 2) provided a direct insight to the rotor limiting process. It also allowed the rotor aerodynamicist, for the first time, to design a rotor blade for the details of the span-wise distribution of aerofoil section properties including stall.

Up to that point, the choice of planform area of a helicopter rotor blade had been based on the static $C_{L\,MAX}$ of its aerofoil section at an arbitrary spanwise station near the blade tip. As a result, constant section blades were the rule, although it had been deduced that high lift performance was important mainly in the outboard regions of the rotor blade. Also, there had been no clear understanding of the effect of the dynamic nature of the rotor environment on the stalling of the blade aerofoil sections; in particular, whether static $C_{L\,MAX.}$ derived from steady wind-tunnel tests would continue to apply with the introduction of advanced aerofoil sections of improved performance.

Calculations using the stall flutter model quickly confirmed that blade stall was important outboard, almost to the blade tip extremity, but they also showed that high lift capability could be relaxed considerably inboard. These calculations in conjunction with some innovative flight experiments at RAE Bedford[3] established the confidence required to move to the distributed aerofoil section design approach used for modern UK rotor blades.

To support the new analytical capability, the testing of aerofoil sections in the UK embraced new techniques with aerofoil sections tested routinely under dynamic conditions in a new rig at ARA Bedford[4]. The rig was configured to produce arbitrary pitch and heave motion and both oscillatory and ramp tests could be performed across the entire Mach number and Reynolds number range of full-scale helicopter rotors. Emphasis was placed on ramp

https://doi.org/10.1017/S0001924000007004 Published online by Cambridge University Press

tests since the Beddoes' model suggested that all the required information to represent the aerofoil section could be deduced from simple ramp motion.

The original Beddoes' model for dynamic stalling was developed initially by generalising the oscillatory test results for three aerofoil sections, produced by Boeing-Vertol[5]. The analysis identified a critical angle acting through a time delay under dynamic conditions. The aerofoil would begin the dynamic stalling process if incidence exceeded over the time period taken for the aerofoil to pass through 1·9 chord lengths of the fluid. For the aerofoil sections of the early Boeing-Vertol tests, could be taken as the static stalling angle of the sections, but for higher performance aerofoil sections, it later became clear that α_1 could not be identified directly in static tests. Thus it was necessary to perform more complex dynamic tests in order to quantify the stalling behaviour of a rotor aerofoil section. For rotor design, aerofoil sections could be readily compared in terms of the Beddoes' model by defining a synthetic maximum lift coefficient based on the dynamic stalling angle α_1 the zero-lift angle of the section α_0 and the measured lift curve slope:

$$C_{L1} = C_{L\alpha}(\alpha_1 - \alpha_0) \quad \ldots (1)$$

The model was developed over time, with the introduction of criteria that related α_1 to physical parameters, such as a critical leading edge a velocity gradient or a critical pressure ahead of the shock near the aerofoil nose that could be predicted directly from the aerofoil geometry[6,7]. These criteria were used to predict α_1 and C_{L1} in the original time delay stall flutter model and they were also used directly in the design of rotor blade aerofoil sections. Confirmatory tests continued to be performed in the unsteady rig at ARA.

The leading edge stall criteria were integrated into a second-generation unsteady stall model that moved away from the simple time delay concept to a more elegant representation of unsteady effects based on two time constants: the time constant that describes the wake shedding process that makes lift lag incidence and a further time constant to account for the lag in development of adverse pressure gradients at the leading edge that control stall or shock induced separation. This further lag that accounted for leading edge pressure was actually expressed in terms of a pseudo lift coefficient, to ease the representation of trailing edge separation effects.

The second generation model and its third generation development were far superior in their ability to model combined leading edge and trailing edge separation effects on aerofoil stall. They could reproduce the measured behaviour of advanced aerofoil sections in the wind-tunnel and could correctly model impulsive effects important in rotor noise predictions. However, some of the utility of the original model, important for design purposes, disappeared as the model became a more powerful analytical tool. As a result, design work – the sizing of rotor blades, the selection and design of aerofoil sections and the calculation of rotor design loads, continued, using the original simple model with conservative but agile supporting assumptions.

This approach was at the heart of the design process that generated the British Experimental Rotor Program (BERP) Lynx and EH101 main rotor designs. The accuracy of the unsteady aerofoil model incorporated in the rotor load and performance calculations was responsible for the excellent agreement achieved between predicted and demonstrated flight envelopes and overall performance and loads. But from the design point of view, it was the physical understanding derived from the unsteady stall models that was of paramount importance, underpinning the design strategy and reflected in the resulting blade design configurations.

https://doi.org/10.1017/S0001924000007004 Published online by Cambridge University Press

2.2 Time delay model for leading-edge separation

The important features of the original time delay model for rotor design are outlined in Fig. 1. The aerofoil sections on which the time delay model was initially based all exhibited leading-edge separation, therefore the time delay model is applied most easily to this type of section. The model represents the aerofoil section in terms of thin aerofoil theory extended to the dynamic situation using an indicial approach. The aerofoil section representation is therefore compatible with conventional aerofoil section design methods as developed by NACA[8].

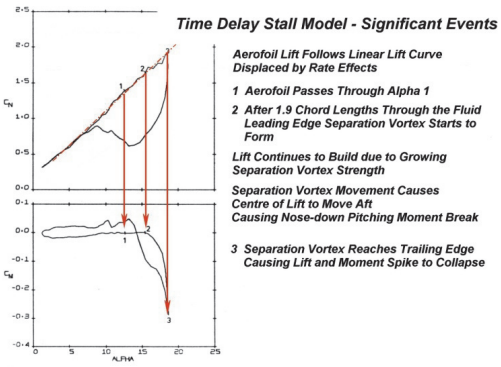


Figure 1. Important features of the time delay leading edge separation model.

The aerofoil is assumed to have a linear lift curve slope with a defined zero-lift angle α_0 and a stalling angle α_1. In dynamic conditions the lift follows the static lift curve slope, displaced by dynamic effects associated with the geometry of the motion and changes in incidence induced by the vorticity shed continuously into the wake in response to the changing aerofoil section lift. The example of Fig. 1 is for oscillatory motion, but for ramp motion at constant angular velocity, the shift in the linear lift curve slope simply settles to a constant value, dependent on the ramp rate (Appendix 1).

As incidence increases, the aerofoil follows the linear lift slope and the pitching moment remains small, made up of the static attached moment terms due to camber and any offset of the aerodynamic centre from the ¼ chord position, plus attached flow rate effects. In the original model, these rate effects were simply adopted from Theodorsen's harmonic analysis[9] and were based on the aerofoil section pitching motion, as opposed to the dynamic variation of its incidence. The second and third generations of the model changed the attached flow moment formulation to allow for incidence change effects, mainly to accommodate blade-vortex interactions.

As α_1 is exceeded, the model assumes that there are initially no deviations from the attached flow lift or moment trends. In unsteady wind-tunnel tests, reversals of flow are seen to occur within the upper surface boundary layer of the aerofoil section, but these do not change the outer flow field that determines the aerofoil pressure distribution and the resulting integrated force and moment. This situation is assumed to continue until a point equivalent to the time taken for the aerofoil section to pass a set distance through the fluid (1·9 chord lengths) after which, the stalling process quickly develops. This apparently universal time delay to the stalling process, discovered through inspection of hundreds of oscillatory test cases by Beddoes[1], is the basis of his simple dynamic stall model.

After the time delay is exceeded, the lift continues to build following the attached flow curve, but the moment begins to diverge rapidly to a nose down peak. The corresponding flow pattern involves the appearance of a detached vortex over the forward upper surface of the aerofoil section, fed by the separating boundary layer. After the appearance of this vortex, the aerofoil lift is made up of a combination of bound circulation effects and vortex lift from the separation vortex, which grows in strength as incidence continues to increase. The increase of the total lift depends on the sum of the two lift sources and its continued linear variation is somewhat fortuitous. Dynamic tests at low Mach number at Glasgow University and elsewhere show

https://doi.org/10.1017/S0001924000007004 Published online by Cambridge University Press

distinct spikes in the total lift just before the vortex crosses the aerofoil trailing edge into the wake and the lift collapses. However, at typical helicopter rotor Mach numbers, the linear assumption of the original time delay model appears to be accurate enough.

The change in pitching moment comes from the shift of centre of lift from near the ¼ chord position to its position for fully separated flow at about 40% chord. The onset of this shift is associated with the movement of the separation vortex down the aerofoil upper surface as it grows in strength. The pulse of moment is associated with the lift of the vortex travelling toward the trailing edge. Its speed of movement seems to be at about ⅓ of the free stream velocity. The vortex lift collapses as the vortex crosses the aerofoil trailing edge, leaving the lift due to bound circulation of the fully separated flow alone. The speed of propagation of the vortex over the chord leads to another effective time delay of about three chord lengths through the fluid between the moment break and the lift collapse. After the vortex departs from the aerofoil trailing edge the pitching moment subsides to the product of the fully separated flow lift and the offset of the aerofoil centre of lift which settles at about 40% chord.

The simplicity of the model makes it very easy to use in design situations and to guide the analysis of aerofoil section test data. For example, critical angles for moment and lift breaks measured in ramp tests for an aerofoil section displaying the most straightforward type of stalling behaviour, a sharp separation from the leading edge, are summarised in Fig. 2. Also shown are the slopes implied by the expected time delays. The stalling angle is found by extrapolating back to a pitch rate of zero and may be used directly for design purposes.

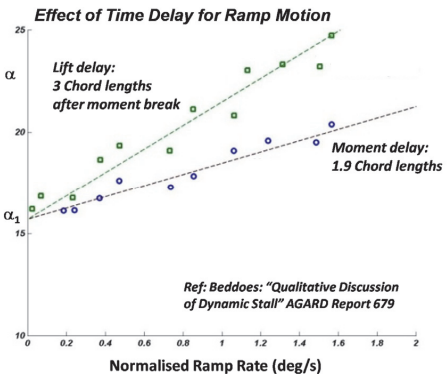


Figure 2. Identification of for the simple time delay model from lift and moment breaks in ramp tests.

Not all aerofoil sections exhibit such straightforward stalling behaviour. Appendix 2 contains an analysis of individual lift and moment ramp time histories for RAE 9651 a rotor aerofoil section exhibiting a particularly complicated stalling behaviour. The appendix shows how the critical angles are identified and a summary of the results is presented for a range of practical Mach numbers. Although the procedures may appear somewhat arbitrary, experience has shown that they produce very consistent results. Comparison of the results with the generalised engineering model enables powerful insights into the physical stalling behaviour of the aerofoil section to be deduced.

2.3 Leading-edge criterion

After the establishment of the time delay model, which initially amounted to simplify a synthesis of unsteady aerofoil section test data, one of the first tasks was to investigate whether stall onset could be predicted directly. This work eventually led to the second and third generation unsteady stall models but also generated tools and insight that could be used directly in design.

Most helicopter aerofoil sections in use at the time, exhibited a clear leading-edge stall, or in the case of thicker sections such as NACA 0012, the influence of trailing edge separation,

https://doi.org/10.1017/S0001924000007004 Published online by Cambridge University Press

although apparent in the data, was fairly minor in importance. It was, therefore, natural to look for a leading-edge separation criterion, applicable at low retreating blade Mach numbers. One such criterion was defined by Evans and Mort[10].

The leading edge criterion is an empirical rule. Evans and Mort performed a rather elegant theoretical analysis in which they derived the parameters that would be likely to control flow breakdown near the leading edge of a two-dimensional aerofoil section, assuming a turbulent re-separation process. They then performed theoretical calculations to estimate these parameters for a wide range of aerofoil sections that appeared to exhibit leading edge (sudden) stall in the static tests that made up the large NACA database. Their analysis indicated that the controlling parameters were the distance along the aerofoil surface traversed by the boundary layer decelerating from a peak velocity near the aerofoil leading edge and the magnitude of the deceleration (proportional to the peak velocity).

In order to avoid complications in the calculations due to the representation of the aerofoil curvature right at the leading edge, they defined an arbitrary pair of velocities as shown in Fig. 3 for their calculations. The flow about the individual aerofoil sections at their stalling points was calculated using an incompressible and inviscid model, and the resulting values of the peak velocity and distance were allowed to define the correlation. It is important to note that no attempt was made to represent the flow details – boundary layer, separation bubbles or turbulent transition – in the flow calculations. All these details lay in the experimental data and did not need to be calculated explicitly.

To extend this technique to the helicopter case, an incompressible, inviscid two-dimensional aerofoil section flow calculation model based on a panel representation of the aerofoil was employed to generate velocity and distance information. Because the Mach number range of the available UK data was higher than that of the standard NACA low speed database and it was intended to apply the results at typical helicopter retreating blade Mach numbers, a simple compressibility correction developed by Wilby[11] was employed to adjust the local Mach numbers, which could rise well above unity near the leading edge at $C_{L\,MAX}$ for a free stream Mach number of 0·3.

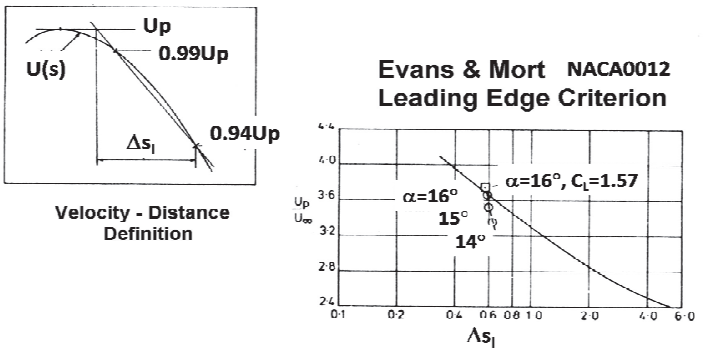


Figure 3. Evans and Mort leading-edge stall criterion.

This adjustment was based on local velocity alone, and therefore, could not represent shocks, but for the cases in question, shocks and isentropic recompression are almost indistinguishable and in any case a velocity distribution with a discontinuity would have made the Evans and Mort's technique difficult to apply. The criterion line was re-calculated using UK data and the original correlation curve was confirmed. The example for NACA 0012 is shown in Fig. 3.

https://doi.org/10.1017/S0001924000007004 Published online by Cambridge University Press

Several useful observations and applications emerged from the correlation process.

First, to correlate the velocity distribution near the aerofoil section leading edge, it was insufficient to simply match the test incidence. A panel method applied to an aerofoil section of finite thickness will produce a lift curve slope that overestimates test values by as much as 20%. The problem lies in the failure to predict the effect of the boundary layer on the effective shape of the aerofoil section. In the inviscid calculation, the flow leaves the trailing edge at the mean angle of trailing-edge surfaces. In practice this flow angle is never achieved, because the boundary layer acts to alter the angle at which the flow leaves the trailing edge.

However, the panel method allows the incidence and the lift both to be specified, allowing the experimental lift-incidence characteristic to be followed exactly. In the panel calculation, there is generated an implied singularity as the flow rounds the sharp trailing edge, making the local flow solution in the vicinity of the trailing edge quite unrealistic. Near the trailing edge, but further away from the surface, the effect is simply to change the deflection the angle of the flow. At the aerofoil nose, the effect is to change the magnitude of the leading edge velocity but not the shape of its distribution. Therefore, specifying both lift and incidence is an effective way to produce a realistic velocity distribution near the aerofoil nose.

This technique allowed the leading edge stall correlation to be extended to cases where there was clear evidence of local trailing edge separation in the prominent rounding of the lift curve prior to final stall. Matching both lift and incidence usually produced points that agreed closely with the leading edge criterion line and confirmed that the stalling process of these aerofoil sections, although influenced by the trailing edge separation, was ultimately caused by leading edge turbulent re-separation.

A useful rule that resulted from these calculations was that the rate of increase of leading edge velocity as the aerofoil followed its linear attached flow lift curve was twice the rate at which it increased when lift was held constant with increasing incidence. This ratio allowed for very simple corrections to the stalling incidence of an aerofoil to remove the effect of trailing edge separation from test data.

One final observation emerged from the correlation studies: The path followed by the peak velocity-distance characteristic with incidence was very shallow for some aerofoil sections. Their characteristics approached the Evans and Mort limit at a very shallow angle, implying a lack of margin to separation for these aerofoil sections over a wide range of incidence. Also, for some aerofoil sections the intersection of their velocity characteristics with the correlated limit curve occurred well to the right on the diagram, challenging the characterisation of the criterion as applying solely to leading edge stall. The general leading edge criterion appears to apply to limiting separations that occur at large values of Δs_l, implying that the critical point can be well aft of the leading edge. The critical point is reached before extreme velocities can make their appearance at the leading edge of these aerofoil sections. However, the resulting stall is as sudden as if the critical condition were close to the aerofoil leading edge. The main BERP blade lifting aerofoil section, RAE 9645, falls into this category.

2.4 Trailing-edge separation effects

Trailing edge separation has a powerful effect on many two-dimensional aerofoil sections, even in dynamic conditions. An example of the effect of trailing edge separation is shown in the behaviour of RAE 9651, a section designed for use at rotor blade inboard stations and used on the EH101 (Fig. 4). This figure has been widely presented as an illustration of the need for dynamic testing of aerofoil sections.

https://doi.org/10.1017/S0001924000007004 Published online by Cambridge University Press

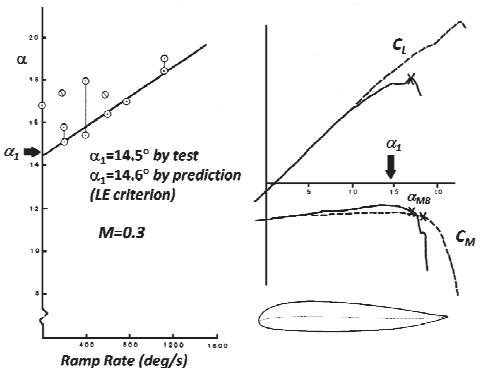


Figure 4. Need for dynamic testing – effects of trailing-edge separation.

Figure 4 presents an analysis of the moment break stalling angles of the aerofoil under ramp-up motion at various rates (see also Appendix 2). Superimposed on the figure is the moment break angle derived from tests performed under quasi-static conditions, as well as the predicted value for α_1 according to the leading edge criterion method. A couple of typical quasi-static and ramp case lift and moment histories are illustrated to the right and the moment break angles are plotted against the ramp rate on the left.

The quasi-static results were derived from high amplitude oscillatory tests performed at a frequency low enough that rate effects could be considered negligible. However, unlike steady tests, they were quick enough to avoid the settling of the flow pattern into an unrepresentative situation where the trailing-edge separation is given the time to spread spanwise across the wind-tunnel, maximising its effect, but not necessarily relevant to the rotor situation.

As discussed in Appendix 1, ramp motion should produce a linear increase in lift with pitch angle. The time histories show that this is the case except at higher incidences where the characteristic rolling over of the lift curve usually associated with trailing-edge separation intrudes. This effect is much reduced for the high rate case.

Appendix 1 also shows that the moment break angles for leading edge stall aerofoil sections, which are well described by the original time delay model, should increase linearly with ramp rate and indeed a straight line can be used to represent the lower boundary of the stall data in Fig. 4. This limit line coincides with the moment break angle variation implied by the time delay stall model in conjunction with the leading-edge criterion prediction of α_1. It is reasonable to assume that the limit line would define the stalling of the aerofoil section, if it exhibited a purely leading edge stalling behaviour.

However, at lower ramp rates the aerofoil section can exceed the leading edge stall limit by a considerable margin. The physical explanation for this behaviour involves trailing edge separation, which reduces the angle at which flow leaves the aerofoil at the trailing edge, reduces the circulation and relieves the adverse pressure gradient at the leading edge that causes ultimate flow breakdown. As a result, the aerofoil section can reach a much higher angle before the moment breaks.

The prominence of trailing-edge separation in the stalling process of this aerofoil section and of many high-performance aerofoil sections for helicopter use prompted the inclusion of its effect in the second and third generation versions of the dynamic stall model[7]. Trailing edge separation was modelled by means of the simple Kirchhoff approach that related the aerofoil section lift to the chord-wise position of a separation point on the aerofoil rear upper surface. As incidence increases, the separation point tends to move forward from the trailing edge and the separation bubble behind it tends to grow. The trailing-edge separation point is treated as an independent dynamic variable with its own time constant in the second and third generation models.

The time constant of the trailing-edge separation tends to be much greater than the time constant governing the separation process at the leading edge of the aerofoil section. Therefore as ramp rate increases, the extent of trailing-edge separation tends to reduce because it does

https://doi.org/10.1017/S0001924000007004 Published online by Cambridge University Press

not have time to develop before the aerofoil stalls from the leading edge. This trend is apparent in the data of Fig. 4, where as ramp rate increases, the overshoot of the moment break angle reduces until the stall can be defined by the leading edge criterion alone.

Therefore, at low rates when a progressive trailing-edge separation occurs, there can be a beneficial effect on the aerofoil dynamic stalling angle. This effect is deduced using the unsteady stall engineering model to structure complex experimental data and to identify the apparent trend, which would be otherwise hidden in the complex data. Whether the beneficial effects of progressive trailing edge separation apparent in wind-tunnel result read across to the rotating environment is another question.

2.5 Sudden trailing-edge stall

Using the original time delay model to analyse the stalling behaviour of some other high performance aerofoil sections reveals another complication in accounting for stalling behaviour. The ramp test moment break angle data and quasi static and static test data for the RAE 9645 aerofoil, the main lifting section of the BERP Lynx and EH101 rotor blades, is plotted in Fig. 5. Superimposed on the figure is a line with the slope suggested by the time delay model for the leading edge stall of 1·9 chord lengths through the fluid, adjusted to best fit the data.

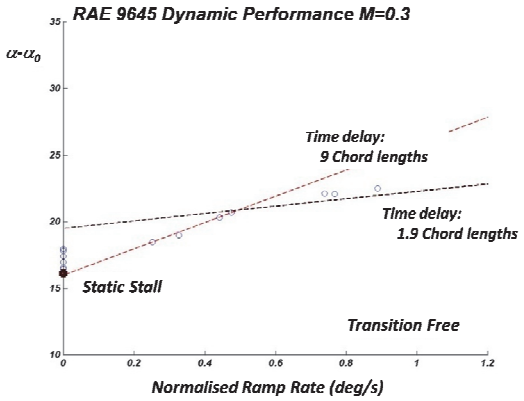


Figure 5. High performance aerofoil sections displaying sudden stall but not completely described by the original time delay model for leading-edge stall.

As with RAE 9651, the time delay model fits best at high angular rates, but the characteristic of this aerofoil and many other cambered aerofoil sections used in advanced rotor designs differs markedly from that of the thicker aerofoil. At low ramp rates, moment breaks occur at angles much lower than the intercept value of the leading edge stall line suggested by the time delay model. A line of much steeper slope produces a good fit to this lower rate data and also appears to coincide with the moment break angle of the static stall. This feature is present in the behaviour of most of the aerofoil sections of moderate thickness tested at ARA, although it is most prominent in RAE 9645 aerofoil. It was reported by Wilby[4] and is also apparent in the results of most of the aerofoil sections tested at the University of Glasgow[12].

RAE 9645 exhibits some rounding of the lift characteristic as the stalling angle is approached, but the stall remains quite sudden – suggesting a simple leading edge stall mechanism for the final flow breakdown. However, in calculating the leading edge velocity profile parameters to predict the stall using the leading edge criterion for RAE 9645, it was noticed that the characteristic crossed the criterion boundary at a very high value of the distance parameter Δs_l with a correspondingly low peak velocity. In fact the aerofoil limited at an incidence well before the sharp leading-edge velocity peak and critical adverse velocity gradient so prominent in the velocity distributions of conventional helicopter aerofoil sections could begin to develop. The prediction of the stalling angle was accurate, so it appeared that the leading-edge criterion not only predicted stalling that originates in the adverse velocity gradients at the extreme leading edge of aerofoil sections, but also sudden stalls that originate in the flow well aft of the leading edge.

https://doi.org/10.1017/S0001924000007004 Published online by Cambridge University Press

Figure 5 suggests that there is more than one physical process that can cause a moment break with the sudden characteristic of a simple leading edge stall. Moreover, this behaviour is present in most advanced high-lift helicopter rotor aerofoil sections. The low rate data in Fig. 5 is somewhat sparse but it is entirely consistent with the results for other aerofoil sections measured in great detail at the University of Glasgow and included in their recent version of the unsteady stall model[12].

Taking a pragmatic approach to the definition of α_1, a best-fit line through the lower rate data may be generated by using the simple time delay approach, resulting in a time delay equivalent to nine chord lengths through the fluid as shown in Fig. 5. This line also intersects the static stall angle. Such a long time delay is obviously not consistent with the time delay of the original leading-edge stall model. It is consistent, however, with the time scales associated with the development of separated flow at the trailing edge. Its behaviour is quite different to the trailing edge separation displayed by RAE 9651. It does not alter the lift of the aerofoil or modify its circulation to allow the leading edge to reach a higher angle prior to stalling. It produces a sudden stall of itself, before the leading edge can reach critical conditions.

Other sudden stalls known to be associated with rear separation have been observed. With RAE 9648 section, the flow over the entire mid-rear upper surface could break down suddenly. RAE 9648 was the section used at inboard stations on the Lynx BERP III blade and it was with these blades that a Lynx aircraft set the helicopter world speed record in 1986. In wind-tunnel tests the section could achieve a stalling angle consistent with the leading edge criterion of about 15º, but every now and again it would stall at 11º.

It turned out that this effect was produced by the design of the section. In an attempt to produce a reflex aerofoil section with a positive zero-lift pitching moment starting with RAE 9645, the outboard high-performance section, the ordinates of the rear upper surface alone were reduced. As a result, increased adverse surface curvatures were introduced in the rear upper surface aft of the aerofoil crest and the flow aft of about 30% chord could suddenly separate. The process was quick enough to appear like a leading edge stall. A modified section RAE 9683, was designed for the subsequent production Lynx BERP blade with its rear surfaces reconfigured to remove this early separation effect. It maintained the same aft camber line as RAE 9648 but did so by replacing the dell in the upper surface of RAE 9648 with a swelling of the lower surface. Tests showed that this aerofoil could achieve the stalling angle of 15º consistently.

Therefore, there appear to be two distinct types of separation aft of the leading edge:

1. separation at or near the trailing edge itself that generates a separation bubble acting to reduce the circulation for a given incidence angle and allowing the aerofoil section to achieve a higher incidence before it finally stalls from the leading edge – at least in the wind-tunnel. Pitch rate suppresses this effect since trailing edge separation takes a relatively long time to develop in a dynamic situation.
2. Sudden separation from well aft of the leading edge that can produce characteristics similar to a leading-edge stall before the leading edge itself reaches critical conditions.

Each must be dealt with pragmatically when selecting aerofoil sections, sizing blade area or producing design loads. These effects were buried in the test data but were deduced by means of a broad comparison with the engineering model for unsteady stall.

2.6 Design considerations

The existence of rear separation on an aerofoil has a profound effect on its stalling performance, especially in the region of moderate rates of change of pitch or incidence appropriate to the initiation of stall on the helicopter retreating blade. It should be remembered that in retreating blade

https://doi.org/10.1017/S0001924000007004 Published online by Cambridge University Press

stall, the moment pulse and not the actual retreating blade lift is of importance. The moment pulse drives the stall flutter motion that limits the rotor but the rotor thrust is produced mainly fore and aft where the blade remains un-stalled. A rear separation that could reduce the aerofoil circulation and thus allow the aerofoil to reach a higher incidence before the leading edge becomes critical could provide a large advantage – provided the rear separation developed in the rotor environment as it did in the wind-tunnel.

In the development of the BERP blade, many advanced high performance aerofoil sections were tested. Most of these sections displayed some form of rear separation. The need to model the effects of trailing edge separation lead to the development of the second and third generation aerofoil dynamic stall models. In the mean time, the possibility of rear separation had to be acknowledged and accounted for in the design of the BERP blade.

Rear separation played a very large part in the high incidence capability of some of the most attractive candidate aerofoil sections. In particular, the stalling incidence of the low moment section RAE 9647 was nearly as high in the wind-tunnel as RAE 9645, the section ultimately chosen for the outboard stations on the blade[4]. RAE 9645 had a high zero lift pitching moment that required an inboard region of reflex camber to compensate for it. The low moment RAE 9647 would not have required a balancing section inboard, but a progressive trailing-edge separation was integral to its high incidence performance. If this separation did not occur or was modified in the rotating environment, the high performance of the section measured in the wind-tunnel would disappear. It was for this reason that RAE 9645 was ultimately chosen.

In fact for conservative rotor design purposes, blade area sizing, aerofoil section selection and the calculation of fatigue and limit loads, the effects of trailing-edge separation were discounted and the dynamic stall model along with the analysis techniques outlined above and in Appendix 2 enabled this easily to be done. Although the dynamic stall model was developed to account for the trailing-edge separation effects seen in the wind-tunnel tests, design calculations continued to be based on the original time delay dynamic stall model with its assumption of a sudden stall.

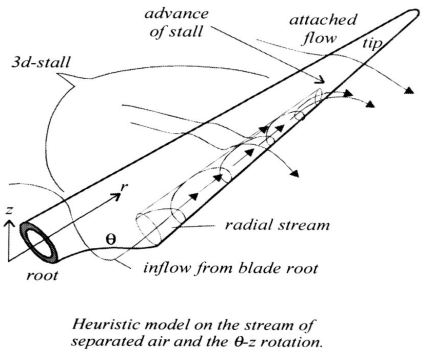


Figure 6. Development of 3D trailing-edge separation and radial flow on a wind turbine blade[14].

At the time this approach was contentious because it could not be demonstrated why the benefits of progressive trailing-edge separation would not read across to the rotating environment. The design decision amounted to a cautious hunch. Recently, however, experience in the wind-turbine field[13] has shown that a rear separation on a rotating blade is profoundly changed by the rotating environment, producing a span-wise flow that modifies the aerodynamic behaviour not only at the blade station in question but affects other stations as well.

Starting from the fundamental fluid flow equations, Corten[13] develops an argument for the existence of the three-dimensional flow pattern shown in Fig. 6. This pattern has been identified experimentally and is cited as the reason for the failure of wind turbine speeds to be reliably governed by means of passive blade stall. As a result, wind turbines require blade feathering systems to prevent them from over-speeding in high winds.

https://doi.org/10.1017/S0001924000007004 Published online by Cambridge University Press

To paraphrase the Corten's physical argument: If a separation develops at the trailing-edge of a non-rotating aerofoil section, it forms a separation bubble of slowly re-circulating flow over its upper rear surface extending downstream beyond the trailing edge. The fluid within this bubble is almost stationary with respect to the aerofoil. It is the presence of this bubble that modifies the effective shape of the aerofoil section and changes its circulation. However, if the aerofoil section is rotating about a rotor shaft, it is following a curved path and so must the fluid in the attached rear separation bubble. This fluid must experience a resulting centripetal acceleration and centrifuge outward. Drawing fluid out of the separation bubble by means of this radial centrifugal pumping must act to reduce the bubble size and increase the rate of rotation of the fluid within, affecting the flow deflection angle at the trailing edge and changing the velocity distribution at the leading edge.

In the helicopter rotor, radial pumping would reduce the effect of the bubble, increasing leading edge velocities and causing the aerofoil to stall at a lower angle than in the non-rotating wind-tunnel environment. The radial pumping effect has not been quantified for helicopter applications but it is very important in wind turbines. Radial pumping depends on the centripetal acceleration of the flow and for a given tip speed, its effect becomes relatively more important as the size of the rotor reduces. If the effect is important for wind turbines, it must increase in importance as the scale of the rotor reduces to a typical helicopter size.

The radial pumping effect will be present wherever the flow acquires the speed of the aerofoil surface, such as in the sub-layer of the blade boundary layer. However, it only becomes important when large volumes of fluid form separation bubbles that alter the effective shape of the aerofoil section. The trailing edge separation bubble is probably the most important instance of this effect, but it could also occur in the case of a shock-induced separation, where the shock triggers a separation bubble and the shape of the bubble relieves the severity of the shock, allowing a higher free stream Mach number to be attained before the flow finally breaks down. If radial pumping reduces the size of the bubble flow breakdown could occur at a lower Mach number relative to wind-tunnel tests or two-dimensional calculations.

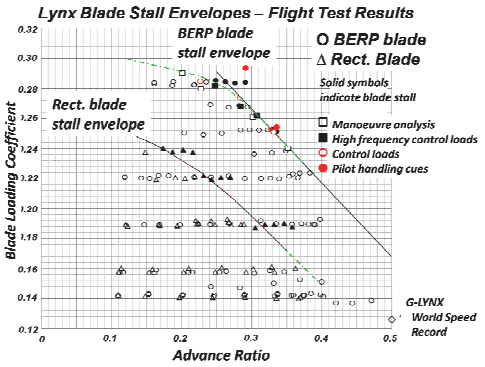


Figure 7. Rotor blade stall flutter envelopes – standard rectangular and BERP blades stall flutter model with supporting flight test points.

Much more needs to be known about radial pumping and rotational effects in the helicopter context, but the decision to remove the effect of the trailing edge separation from helicopter rotor design calculations, appears to have been prudent with hindsight. The good correlation achieved between the theoretically predicted rotor blade stall envelope and that demonstrated in the BERP III flight test program (Fig. 7) was based on an aerofoil stall model where the effect of trailing edge separation had been removed.

2.7 University of Glasgow unsteady stall model

Good engineering models continue to evolve, becoming less empirical as more physical criteria are adopted and more capable of extrapolation with confidence. Since they are continually compared and revised they tend to become the engineers running summary of his understanding

https://doi.org/10.1017/S0001924000007004 Published online by Cambridge University Press

of a problem. Glasgow University has for many years produced excellent experimental data on unsteady stall and has continued research into generalised modelling of the stalling process. Recent developments in these models, which are closely related to Beddoes' third generation model seem to offer benefits with respect to the design applications mentioned above. Its features include:

- Leading-edge separation model that is based on incidence rather than a lagged C_N.
- More general treatment of the development of trailing edge separation without surrendering the simplicity of the original Beddoes' formulation.
- Similar approach to the movement of the centre of lift during the stall process as the original time delay model, which improves accuracy without degrading the utility of the model when used in the design process.
- Improved flow re-attachment model.

The new model has been correlated against the dynamic performance of a variety of wind turbine aerofoil sections tested at low Mach number at Glasgow University. Recently, the model has been successfully correlated in detail against RAE 9651 data at Mach numbers appropriate to helicopter operation[12]. This aerofoil section is a good subject for such an evaluation since its behaviour contains so many interesting features – especially the effects of trailing-edge separation, which persist even at the higher Mach numbers. The correlations of reference 12 of course concentrate on the details of the many individual time histories of stalling events, but the application of the model to the rotor design problem needs to be considered as well.

For design applications, the same uncertainty with respect to trailing edge separation effects identified above still applies. If the model is to be used in helicopter rotor design applications, a means of suppressing the trailing edge separation needs to be identified. Since trailing-edge separation is treated as an independent variable in the unsteady stall model, it must be disabled for design calculations.

The new leading-edge stall criterion – really a synthesis of ramp test results, rather than a prediction of stalling angle from the aerofoil section geometry like the leading-edge criterion – contains two limit lines with different slopes and different intercepts on the axis of zero ramp-rate. This behaviour was discussed above in conjunction with Fig. 5. It was argued that there were probably two physical limitation processes, one involving flow separation driven by the adverse pressure gradient at the leading edge and another driven by the gradient further aft. This second process has a different and larger effective time constant or time delay, but still involves a sudden stall.

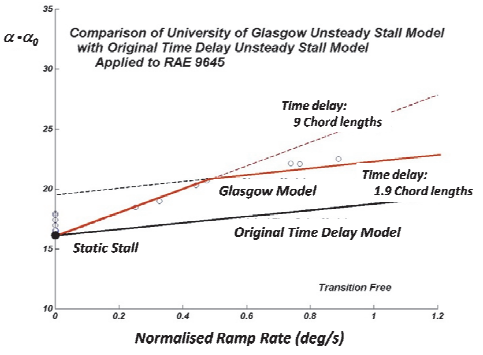


Figure 8. Comparison of Sudden stall criteria between original Time delay model and University of unsteady stall model.

The separation with the longer time delay appears to be predicted by the leading-edge criterion and as long as the associated separation process does not involve a large separation bubble, which would be affected by the radial acceleration field of the rotor, it probably reads across from the wind-tunnel to the rotor without any need for modification.

https://doi.org/10.1017/S0001924000007004 Published online by Cambridge University Press

Figure 8 shows the difference between the direct use of the new Glasgow separation criterion applied to RAE 9645 and the way this aerofoil section was represented in design calculations for the BERP Lynx and EH101 blade using the original time delay stall model. It is possible that all of the important design cases that set the blade area of the rotor involve low enough rates of change of incidence at the stalling point, that the differences between the models are not important, but the new Glasgow model would show a slightly higher performance than the original time delay model for this aerofoil section and for many others. It would probably be safe to take this higher performance into account for rotor design.

The unsteady stall models that developed from Beddoes original work are all traditional engineering analysis models, which are fairly straightforward to invert and apply to design problems as discussed in this paper.

3.0 CONCLUSIONS

The application of aerofoil section dynamic stall models to the design of advanced rotors in the UK has been outlined.

While the dynamic stall model continued to be developed to include more and more complex physical processes, the original time delay model for the sudden leading-edge stall continued to be used for design purposes.

Trailing-edge separation, apparent in the stall of advanced aerofoil sections tested in the wind-tunnel, was identified as feature that might not read across directly to the rotor situation and was discounted in the design process.

Recent physical reasoning indicates that this conservative design approach was justified since flows with large separation bubbles may not read across directly to the rotating environment.

The new University of Glasgow unsteady stall model has been considered in the light of this design practice and suggestions for the use of the new model in design situations have been identified.

The stalling behaviour of an example aerofoil section has been analysed with the aid of the original time delay stall model to identify its stalling performance and related issues.

The engineering model for unsteady stall of an aerofoil has been shown to be a powerful tool for design, analysis of data and for the identification of important physical phenomena for future detailed study. This will continue to provide a practical and effective rotor design tool.

4.0 RECOMMENDATIONS

The importance of separation bubbles in rotating flows has been identified but beyond a technique to ensure that apparent advantages from these bubbles do not produce over-optimistic design decisions, there is no model for the effect of the bubble in the rotating environment of the rotor.

Fundamental research on the effects of the rotating environment of the helicopter rotor on trailing edge separation bubbles and bubbles at the foot of shock waves is therefore recommended because these effects certainly exist and may be important in the behaviour even of existing rotors.

https://doi.org/10.1017/S0001924000007004 Published online by Cambridge University Press

DEDICATION

We, the authors, would like to dedicate this paper to Tom Beddoes, for what he taught us, among many things, the importance of engineering modelling must be based on physics and not only on numerical solutions. Tom passed away in January 2012 and will be missed greatly by his friends and colleagues.

REFERENCES

1. BEDDOES, T.S. A Synthesis of Unsteady Aerodynamic Effects Including Stall Hysteresis European Rotorcraft and Powered Lift Forum Southampton, 1975.
2. BEDDOES, T.S. Retreating Blade Stall Flutter ARC 36966, Aerodynamics 1976.
3. BROTHERHOOD, P. and REILLY, M.J. Flight experiments on aerodynamic features affecting helicopter blade design, *Vertica*, 1978, **2**, pp 27-42.
4. WILBY, P.G. The Development of Rotor Aerofoil Testing in the UK – The Creation of a Capability to Exploit a Design Opportunity European Rotorcraft Forum, Brighton, UK, 1996.
5. LIIVA, J, DAVENPORT, F.J., GRAY, L. and WALTON, I.C. Two-dimensional Tests of Airfoils Oscillating Near Stall USAAVLABS TR68-13, **1 and 2**, 1968
6. BEDDOES, T.S. Onset of Leading Edge Separation Effects Under Dynamic Conditions and Low Mach Number AHS Annual National Forum, Washington, USA, May 1978.
7. BEDDOES, T.S. Representation of aerofoil behaviour, *Vertica*, 1983, **7**, (2), pp 183-187.
8. ABBOT, I.H. and von DOENHOFF, A.E. *Theory of Wing Sections*, Dover Publications New York, USA, 1959.
9. THEODORSEN, T, General Theory of Aerodynamic Instability and the Mechanism of Flutter NACA Report 496 1935.
10. EVANS, W.T. and MORT K.W. Analysis of computed flow parameters for a set of sudden stalls in low speed two-dimensional flow NASA TND–85, 1959.
11. WILBY, P.G. The calculation of sub-critical pressure distributions on symmetric aerofoils at zero incidence NPL Aero Report 1208, 1967.
12. SHENG, W., GALBRAITH, R.A.McD, and COTON, F.N. A new stall-onset criterion for low speed dynamic stall, *J Solar Engineering*, 2006, **128**, pp 461-471.
13. CORTEN, G.P. Inviscid stall model EWEC 2001, Copenhagen, Denmark, PG2.27.
14. BEDDOES, T.S. Practical computation of unsteady lift, *Vertica*, 1984, pp 55-71, **8**, (1).
15. HUMPHREYS, C. Results of Oscillatory Pitch, Ramp and Drag Tests on the RAE 9651 Section Aircraft Research Association Ltd Model Test Note M161/2 (No date – Tests January-March 1983).

ACKNOWLEDGEMENTS

The authors would like to acknowledge DTIC, UK MoD for funding this study under the contract A/TM/N03501/C014. Thanks are also due to T. S. Beddoes, Professor Galbraith and Dr Sheng of Glasgow University for the many useful discussions.

APPENDIX 1: EXPECTED DELAY IN MOMENT STALL IN RAMP TESTS

The first generation unsteady stall model developed by Beddoes was based on the observation that once the critical angle for stall was exceeded, a delay of about 1·9 chord lengths through the fluid was obtained before the moment break occurred in dynamic conditions. For ramp motion, the stall delay would allow the aerofoil section to reach a higher angle than before the moment broke. That angle would increase linearly with ramp rate. The increase in angle can be predicted using expressions defined in Fig. 14.

https://doi.org/10.1017/S0001924000007004 Published online by Cambridge University Press

There are three components to the increment in stalling angle observed in ramp tests:

(a) The stall time delay is equal to the time required for the aerofoil to pass through 1·9 chord lengths of fluid:

$$\Delta t = 1 \cdot 9 \frac{c}{V} \quad \textbf{[sec]} \qquad \ldots (1)$$

If the aerofoil section ramp rate is constant, its pitch angle increases prior to the moment break by:

$$\Delta\alpha = \dot{\theta}\Delta t = 1 \cdot 9 \frac{\dot{\theta} c}{V} \qquad \ldots (2)$$

(b) Aerofoil section incidence is determined by the flow tangency condition at the ¾ chord position. If the aerofoil is pitching nose-up about the ¼ chord point, there is an increase in effective incidence due to the downward normal velocity at the ¾ chord position caused by the pitch rate. The increased incidence increases the lift and reduces the pitch angle at which the aerofoil stalls.

For small angles, the increment in incidence at the ¾ chord point is given by the ratio of the normal and free stream velocities and the reduction in apparent incidence at the moment break is given by:

$$\Delta\alpha = -\dot{\theta}\frac{c}{2}\frac{1}{V} = -\frac{\dot{\theta} c}{2V} \qquad \ldots (3)$$

(c) Due to the changing lift as the aerofoil pitches, vorticity is shed from the aerofoil trailing edge into the wake parallel to the aerofoil span. This vorticity induces changes in the effective incidence of the aerofoil section, acting to reduce the lift. The effect of each element of vorticity decays with time as it is convected away from the aerofoil but the motion of the aerofoil section ensures that it is continuously being replaced. For ramp motion, the effect is an incremental decrease in effective incidence, which is proportional to ramp rate.

Equations for the change in effective incidence of the aerofoil section are given in Ref. 14.

$$\Delta\alpha_E(t) = K_\alpha \left[A_1 T_1 (1 - e^{-t/T_1}) + A_2 T_2 (1 - e^{-t/T_2}) \right] \qquad \ldots (4)$$

For a large steady ramp motion assume that starting transients have died away (t >> T).

$$\Delta\alpha_E(t) \approx K_\alpha \left[A_1 T_1 + A_2 T_2 \right]$$

$$\text{and} \quad K_\alpha = K_\theta (1 + \frac{c}{2V}) \approx K_\theta = \dot{\theta} \qquad \ldots (5)$$

The time constants are given by:

$$T_1 = \frac{c}{b_1 (1 - M^2) 2V} \quad \textit{and} \quad T_2 = \frac{c}{b_2 (1 - M^2) 2V}$$

$$\Delta\alpha_E = \frac{\dot{\theta} c}{2V} \left[\frac{A_1}{b_1} + \frac{A_2}{b_2} \right] \frac{1}{1 - M^2} \qquad \ldots (6)$$

https://doi.org/10.1017/S0001924000007004 Published online by Cambridge University Press

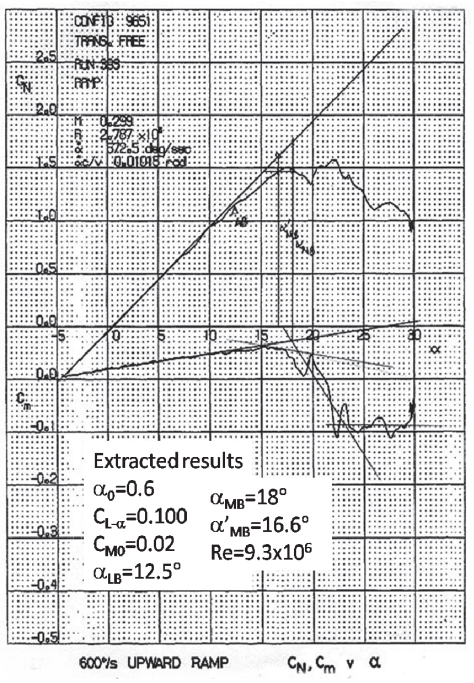


Figure A2.1. Example of analysis of ramp data from ARA test.

where $A_1 = 0{\cdot}165$, $A_2 = 0{\cdot}335$, $b_1 = 0{\cdot}0455$, $b_2 = 0{\cdot}3$

The expected variation of the moment break angle with ramp rate is obtained by summing the increments of incidence due to the time delay, the geometric effect and the shed wake. The expected variation with ramp rate is a straight line that is compared with test-derived values to extrapolate back to the critical angle α_1 at zero ramp-rate.

APPENDIX 2: ANALYSIS OF RAE9651 DATA OF REF. 15

As an example of the analysis required in establishing the performance parameters for an aerofoil, data from the ARA summary report on the tests on RAE 9651 have been analysed in the traditional way. A typical ramp test case is shown in Fig. A2.1.

The analysis pre-supposes the form established by the original time delay model for dynamic stall. Both the lift and moment are idealised as linear functions of incidence during ramp-up motion as expected from linear theory. These idealisations are superimposed on the data plot from the test report[15].

Of interest is the lift curve slope value of this 16% *t/c* aerofoil, which is about 10% below the typical value for a helicopter aerofoil section at this Mach number – indicating a thick boundary layer that modifies the flow deflection angle at the trailing edge even when lift is low. Notice as well that the attached portion of the moment curve has a positive (nose-up) slope, implying an aerodynamic centre approximately 5% ahead of the usual ¼ chord position – another indication of a thick boundary layer at the trailing edge.

The analysis identifies the moment break angle, which is defined by the attached moment idealisation and an idealised straight-line representation of the moment divergence. In drawing the moment divergence for this example, the existence of a high frequency oscillation in the test moment curve has been taken into account in placing the idealisation as a mean through the oscillations.

A feature of the lift time history of this aerofoil is the rolling over of the lift curve at high incidence, a characteristic of gradual trailing edge separation, made more apparent by the linear lift relationship assumed in the time delay stall model.

If it is supposed that the final stall of the aerofoil is governed by leading-edge conditions, a corrected moment break angle removing the effects of trailing-edge separation may be derived as shown. The test moment break angle defines the critical condition at the leading edge. Remembering that the rate of change of leading-edge velocity with incidence when operating on the attached lift curve is approximately double that obtained when lift is held constant, a corrected moment break angle is the mean between the actual break angle and the point on the

https://doi.org/10.1017/S0001924000007004 Published online by Cambridge University Press

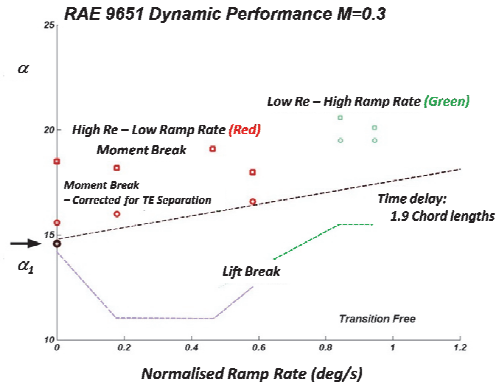


Figure A2.2. Analysis of M = 0·3 data transition free.

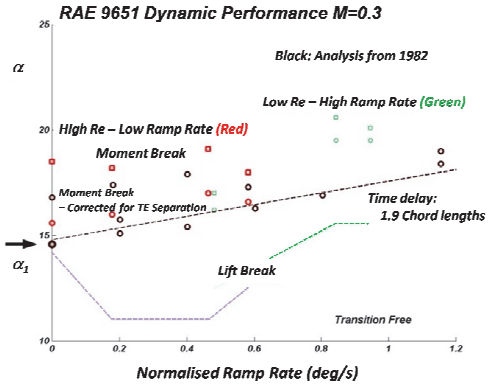


Figure A2.3. Comparison of current analysis with initial estimates M = 0·3.

linear lift curve at the same value of lift. The corrected angle would be the stalling angle of the aerofoil, if for some reason, trailing edge separation failed to develop.

The results of this analysis are plotted along with a limit line with the slope expected from the original time delay stall model – which assumes a leading-edge stall without significant trailing-edge separation in Fig. A2.2. The data when corrected to remove the effects of trailing edge separation conforms to the leading edge stall line fairly well.

Some of the data points in the summary report are obviously corrupted – several of the cases include changes in ramp rate at about the point the aerofoil begins to stall. These points have been corrected or removed but the data remaining is fairly sparse.

The original analysis of RAE 9651 (Fig. 4) is compared to the current analysis in Fig. A2.3. The results are broadly compatible and support the idea that leading-edge stall with no trailing edge relief occurs occasionally even in the wind-tunnel situation. Whether to include trailing edge separation in the design calculations should be carefully considered.

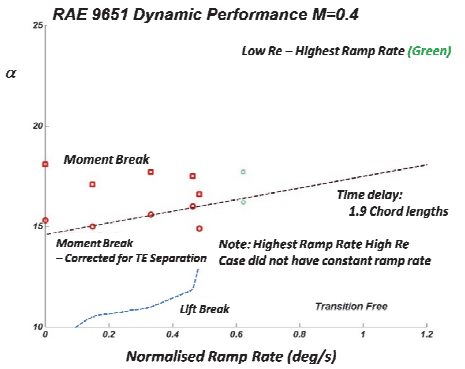


Figure A2.4. Analysis of M = 0·4 Data – transition free.

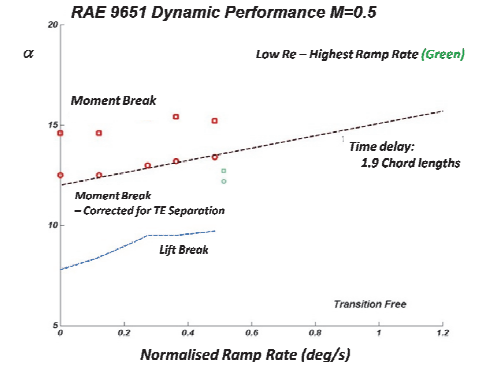


Figure A2.5. Analysis of M = 0·5 Data – transition free.

Figures A2.4 and A2.5 show very similar situations at the higher Mach numbers of 0·4 and 0·5. Transition fixing was introduced as a technique into aerofoil section testing as a means of ensuring that shocks always interacted with a turbulent boundary layer, since for fixed wing applications at high Mach numbers it was difficult to produce a high enough Reynolds number

https://doi.org/10.1017/S0001924000007004 Published online by Cambridge University Press

in the test arrangements available. As long as the boundary layer was turbulent, it was felt that the shock-boundary layer interaction remained realistic. As a result, transition fixing became a feature of aerofoil testing, but its effect on more sensitive problems, like that of aerofoil section stall, was always problematical.

The ARA facility is able to reproduce full-scale helicopter Reynolds numbers and over a range of Mach numbers, therefore free transition became the standard test condition for the helicopter aerofoils. Nevertheless, fixed transition cases were also produced. These are analysed below. The data follows the same trends as the transition free cases, but the corrected moment break angles are slightly lower. There is also less difference between the corrected and uncorrected moment breaks, indicating that transition fixing reduces the extent of trailing edge separation.

A notable exception is the data for a Mach number of 0·5 where the trend with ramp rate deviates significantly from all the other cases and there is a very large reduction in the time delay value required to envelope the data.

The results of the analysis of the transition fixed data are included for interest below in Figs A2.6-8.

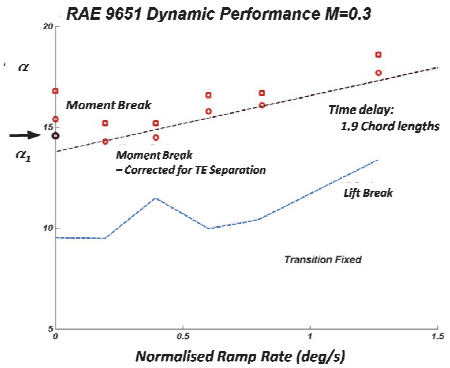


Figure A2.6. Analysis of M = 0·3 data – transition fixed.

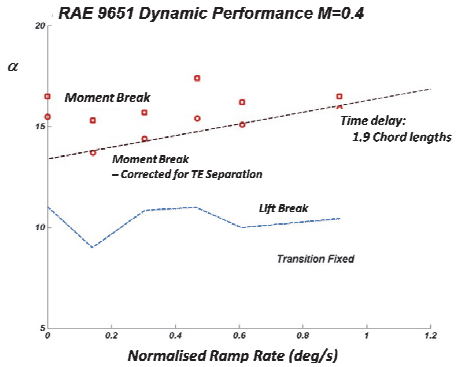


Figure A2.7. Analysis of M = 0·4 data – transition Fixed.

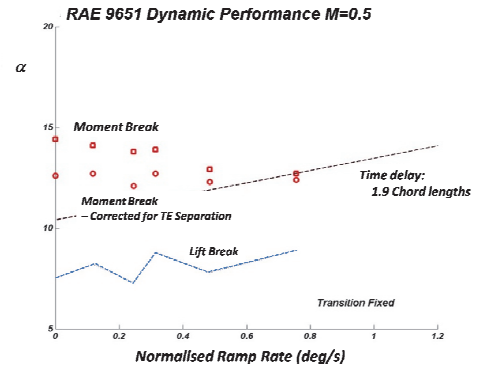


Figure A2.8. Analysis of M = 0·5 data – transition fixed.

https://doi.org/10.1017/S0001924000007004 Published online by Cambridge University Press